

Temperature-Induced Transitions in the Structure and Interfacial Rheology of Human Meibum

Danielle L. Leiske,[†] Christopher I. Leiske,[†] Daniel R. Leiske,[†] Michael F. Toney,[‡] Michelle Senchyna,[§] Howard A. Ketelson,[§] David L. Meadows,[§] and Gerald G. Fuller^{†*}

[†]Chemical Engineering Department, Stanford University, Stanford, California; [‡]Stanford Synchrotron Radiation Lightsource, Stanford Linear Accelerator Center, National Accelerator Laboratory, Menlo Park, California; and [§]Alcon Research, Fort Worth, Texas

ABSTRACT Meibomian lipids are the primary component of the lipid layer of the tear film. Composed primarily of a mixture of lipids, meibum exhibits a range of melt temperatures. Compositional changes that occur with disease may alter the temperature at which meibum melts. Here we explore how the mechanical properties and structure of meibum from healthy subjects depend on temperature. Interfacial films of meibum were highly viscoelastic at 17°C, but as the films were heated to 30°C the surface moduli decreased by more than two orders of magnitude. Brewster angle microscopy revealed the presence of micron-scale inhomogeneities in meibum films at higher temperatures. Crystalline structure was probed by small angle x-ray scattering of bulk meibum, which showed evidence of a majority crystalline structure in all samples with lamellar spacing of 49 Å that melted at 34°C. A minority structure was observed in some samples with d-spacing at 110 Å that persisted up to 40°C. The melting of crystalline phases accompanied by a reduction in interfacial viscosity and elasticity has implications in meibum behavior in the tear film. If the melt temperature of meibum was altered significantly from disease-induced compositional changes, the resultant change in viscosity could alter secretion of lipids from meibomian glands, or tear-film stabilization properties of the lipid layer.

INTRODUCTION

The tear film is a thin fluid that protects the surface of the eye (1). The film is meant to remain continuous at all times to provide visual clarity and to protect the corneal epithelium. However, in some forms of dry eye disease the tear film is unstable, causing it to thin prematurely and subsequently dewet from the corneal surface. Tear-film dewetting produces dry spots on the cornea (1–3). Repeated occurrences of dewetting and exposure of the ocular surface eventually lead to irritation and inflammation (4).

Like many naturally occurring films, the tear film is complex in organization and composition, making stability analysis a challenging problem from a fluid mechanics perspective. The tear film is organized roughly into two layers: nearest the cornea lies a 3–40- μ m aqueous layer rich in mucins and proteins while a 10–100-nm lipid layer forms the interface with the air (5,6). Moreover, >100 mucin, protein, and lipid species have been identified in the human tear film (7), making differentiation between disease groups based on constituent analysis impractical (although comparisons on the relative amounts of proteins or lipids present have been shown to correlate with disease (8)). Finally, correlations between clinical symptoms such as tear-film break-up time, tear volume, and disease severity are often inconsistent between patients (9). With these considerations, it has been difficult to identify the primary causes of tear-film instability.

Much attention has been devoted to studying the lipid layer, as it is thought to play a crucial role in tear-film

stability. Dysfunctions in tear-film lipids, including changes in composition or excretion levels, have been associated with some types of dry eye disease (10–12). Therefore, a number of researchers have focused their efforts on the lipid layer to ascertain whether characteristics such as film thickness or lipid composition can be linked to break-up time, a clinical measure of stability that has been correlated with disease (9,13–15). The majority of lipids in the lipid layer are supplied by the meibomian glands, which are located inside the eyelids. Major components of meibum include long chain nonpolar species such as wax esters, cholesterol esters, fatty acids, and others with varying degrees of saturation (16–18). Despite the recent attention garnered by meibum, physical properties that could influence tear-film stabilization, such as structure and viscoelasticity, remain largely unexplored.

One property of meibum that may be closely linked to performance is melt temperature. As a natural extract composed of a complex mixture of lipids, meibum melts over a range of temperatures rather than at a single temperature. Meibum collected from healthy individuals melts near body temperature as individual hydrocarbon chains in meibum become significantly more disordered when heated from 25 to 40°C (19). In addition, this melt transition temperature changes with age and disease (8,20,21), demonstrating that changes in lipid composition can modify the average melt temperature. As meibum melts, the hydrocarbon chains of the lipids transition from the *trans* rotomers to *gauche* rotomers (19). The increased disorder in the lipids will cause them to pack less densely. Because structured fluids tend to be more viscoelastic than unstructured fluids, subsequent variations in meibum viscosity would alter normal

Submitted August 5, 2011, and accepted for publication December 7, 2011.

*Correspondence: ggf@stanford.edu

Editor: Ka Yee Lee.

© 2012 by the Biophysical Society
0006-3495/12/01/0369/8 \$2.00

doi: 10.1016/j.bpj.2011.12.017

expression of meibum from the glands and/or stabilization properties of meibum on the surface of the tear film. Disruption of meibomian gland expression and modification of lipid viscosity may cause clinically measurable changes in tear-film performance such as shortened tear-film break-up times. Thus, meibum structure and viscoelasticity may be valuable indications of how the physical properties of meibum change near the melt temperature, and ultimately, how these contribute to reduced tear-film stability with dry eye disease. These aspects of meibum behavior within the melt transition have not yet been studied.

We have explored temperature-induced transitions in the structure and mechanical properties of meibomian lipids. The interfacial viscoelasticity was strongly dependent on temperature: the interfacial moduli decreased by several orders of magnitude between 17 and 35°C, which could influence both delivery of the lipids from the gland to the tear film and the mechanical stabilization of the film itself. In addition, Brewster angle microscopy showed that meibum films at 35°C contained micron-sized inhomogeneities that were not present at 24°C, presumably due to increased disorder at higher temperatures. To begin to understand how the structure of meibum changes within this temperature range, small-angle x-ray scattering (SAXS) was used to measure the crystalline structures of bulk meibum. Two types of crystalline phases were identified in most meibum samples; the first melted below physiological temperatures and the second persisted up to 40°C. In addition, the spacings and melt temperatures of these crystalline structures were highly conserved within a control population, suggesting that the lipid species present in such structures are also conserved.

The correlation between melting of crystalline phases and reduced film viscoelasticity near body temperature demonstrates that meibum structure and interfacial rheology are linked. It would appear that like many natural systems, meibomian lipids are tuned to be sensitive to physiological operating conditions; in this case, the lipids undergo a striking transition between low and high viscosity above and below body temperature. Thus, compositional changes that modify the average melt temperature would alter the natural performance of meibum, both in lipid expression and lipid layer performance.

MATERIALS AND METHODS

Sample collection

Before the start of this study, ethics approval was attained and all procedures adhered to the Declaration of Helsinki. Meibum was expressed from the lower lids by applying pressure with a sterile cotton swab against Mastrota paddle. Secreted meibum was collected by gently scraping of the eyelid margin with a small degreased metal ocular spud. Samples collected from the right and left eyes of a single volunteer were pooled and placed onto a small glass coverslip that was then placed in an amber jar for storage at -20°C until use.

Meibum samples were collected from two different sets of subjects depending on the planned analysis. For isotherm, interfacial rheology, and

Brewster angle microscopy data, meibum samples were collected from volunteers (one male and four females), each of whom presented with no complaints of dry eye or obviously inflamed lid margins. For SAXS analysis, only healthy nondry eye, noncontact lens-wearing females between the ages of 34 and 73 (mean age of 56.1 ± 12.8) were sampled. Specifically, a meibum sample was collected if upon exam the volunteer met all of the following criteria: a), lack of dry eye symptoms (<5) as determined by the Schein Questionnaire (22); b), minimal to absence of sodium fluorescein staining in the cornea; c), tear-film break-up time >7 s; and d), absence of meibomian gland dysfunction (MGD) as determined by normal meibum appearance.

Isotherms and Brewster angle microscopy

Meibum was spread on a subphase of Gibco pH 7.4 phosphate buffer saline (Invitrogen, Carlsbad, CA) in a Langmuir mini-trough equipped with symmetric barriers (KSV, Espoo, Finland). Solvent was not used as a spreading agent in attempt to preserve any natural structure present in the lipids upon removal from the glands. To spread meibum without the aid of solvent the trough was heated by a recirculation bath. Surface temperature was monitored with a probe (Madge Tech, Contoocook, NH) placed 1–2 mm below the liquid surface behind the trough barriers to prevent disruption of the lipid layer. Meibum samples from a single individual were spread by touching the lipids to the aqueous surface at temperatures >35°C, when the lipids spread spontaneously. Surface temperatures were kept <37°C to avoid lipid reorganization at temperatures higher than what would be experienced under physiological conditions.

After spreading, meibum was given 30 min to equilibrate before compression of the surface. Surface pressure versus trough area isotherms and film morphology (via Brewster angle microscopy, BAM) were recorded at barrier speeds of 10 cm²/min and 35°C. After one compression, the barriers were opened and the subphase was cooled to 24°C over the period of 1 h. A second compression cycle was performed with the same material. Meibum isotherm hysteresis is minimal between repeated isotherms of meibum films at a single temperature (23); therefore, changes in isotherms are attributed to the temperature of the isocycle.

Interfacial rheology

Experiments were performed in the single frequency mode of an interfacial stress rheometer (ISR) (24,25). An oscillatory magnetic field is utilized to displace a magnetic rod, floating at the air-water interface, thus creating oscillatory shear deformations to material spread at the interface. The instrument is not capable of operating with the range of deformation rates and strains that would be experienced by the tear film *in vivo*, thus it is not meant to model deformations found in the eye. Rather, deformations are applied over strains sufficiently small so as not to disrupt material structure, and results can be used as a metric to compare trends within a sample or different samples to each other.

Samples were spread as described in the previous section. After spreading meibum at 35°C the trough was cooled to 17°C over a period of 1 h before the film was compressed to the desired surface pressure. The trough surface area was held constant as the interface was slowly heated to 35°C at 0.3°C/min. During the heating cycle, the interfacial rheology was monitored at a frequency of 1 Hz and strain of 1.74%, which is within the linear viscoelastic region for meibum. Temperature changes in time were monitored by placing a temperature probe 1–2 mm below the surface behind the trough barriers.

Although the qualitative behavior between samples was consistent, the values of surface viscous and elastic moduli were not quantitatively reproducible (see [Supporting Material](#)). Such variability was observed for samples collected from the same individual on different dates, as well as samples from different individuals. A major factor that could have influenced the variability of results is the amount of meibum added to the trough. Because the interest was in measuring the properties of meibum from

a single donor, a mass of material <0.1 mg, the amount could not be accurately controlled or measured, and may influence the microscale structure of interfacial films. Other factors include differences in meibum from different collection dates from a single individual, or finally, differences between individuals (26). However, the qualitative behavior, dramatic reduction in film moduli between 20 and 35°C, occurred in all samples measured. The lack of quantitative endpoints from interfacial rheology experiments motivated x-ray scattering studies.

SAXS

SAXS experiments were performed at the Stanford Synchrotron Radiation Lightsource at the SLAC National Accelerator Laboratory on beamline 1-4. Samples were mounted between Kapton windows and scattering was collected by a two-dimensional detector for 5-min intervals ($I(q)_{\text{sample+holder}}$). Scattering of the sample holder with Kapton windows ($I(q)_{\text{holder}}$) and dark (closed shutter, $I(q)_{\text{dark}}$) were also recorded. Data from the two-dimensional detector were reduced by integrating the intensity radially. The images were divided into four quadrants and integration was performed between 2 and 88° for each quadrant. Transmission (T) of the holder and sample were measured to normalize intensity and remove scattering volume dependence. Background scattering was removed using Eq. 1 and a baseline fit was subtracted from the data such that background was independent of the scattering vector, q . The scattering vector is related to length scales in real space, d , by the expression $q = 2\pi/d$. Gaussian fits were used to find peak center, width, and integrated intensity:

$$I(q)_{\text{sample}} = \frac{I(q)_{\text{sample+holder}} - I(q)_{\text{dark}}}{T_{\text{sample+holder}}} - \frac{I(q)_{\text{holder}} - I(q)_{\text{dark}}}{T_{\text{holder}}} \quad (1)$$

Scattering of the samples was measured at temperature increments of 2–3°C between 24 and 45°C, although not all samples were heated to 45°C. Samples were no longer heated once the peaks had disappeared. To explore hysteresis, after one heat cycle, three samples were allowed to cool to room temperature over a period of three or more hours at which point SAXS experiments were repeated without disturbing the samples. A fresh meibum sample was collected on-site to confirm that structures and melt behavior were not artifacts of storage conditions.

RESULTS

Isotherms and BAM

The surface pressure versus area isotherms of meibum films was quite different at room temperature compared to 35°C: isotherms showed that meibum compressibility was higher at 35°C (Fig. 1). At the same surface coverage, the maximum achievable surface pressure at 35°C (16 mN/m) was less than that at 24°C (36 mN/m).

Differences in microstructure with temperature were evident in Brewster angle microscopy (BAM) images of the meibum film (Fig. 2). Under all conditions the films were structurally heterogeneous, containing regions of varying brightness on the order of hundreds of microns. The black regions are likely regions with little or no material; surface coverage of these regions decreased upon film compression (Fig. 2, *b* and *d*). At 24°C (Fig. 2, *a* and *b*), the films contained regions with varying intensity. Although such variations in intensity can be caused by local variations

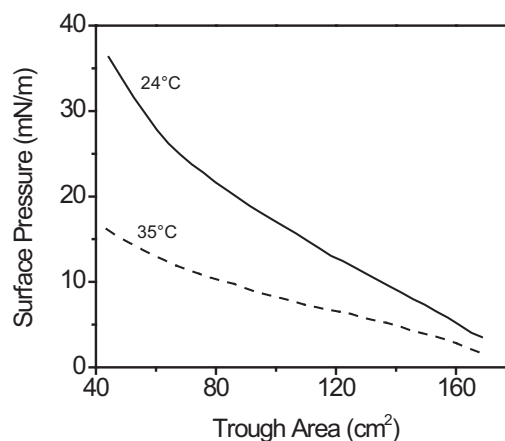


FIGURE 1 Surface pressure versus trough area isotherms of the same meibum sample at 24°C (solid) and 35°C (dashed). The isotherm at 35°C was performed first. After one isocycle, the interface was cooled to 24°C at maximum area before the second isotherm was executed.

in molecular tilt (27), we hypothesize that the brighter regions contain more than one layer of lipid molecules. Thus, the interfacial films studied here were not pure monolayers. Within a region of uniform intensity, the film appeared to be homogeneous within the resolution limit of the BAM (10 μm). In contrast to meibum films spread by chloroform, meibum spread without solvent did not achieve a homogeneous appearance at high surface pressures (28).

Conversely, at 35°C, small-length-scale inhomogeneities are present in the meibum film, resulting in a film that appeared to be textured (Fig. 2, *c* and *d*). These structures persisted when the film was fully compressed with length scales of microns or tens of microns. These inhomogeneities may

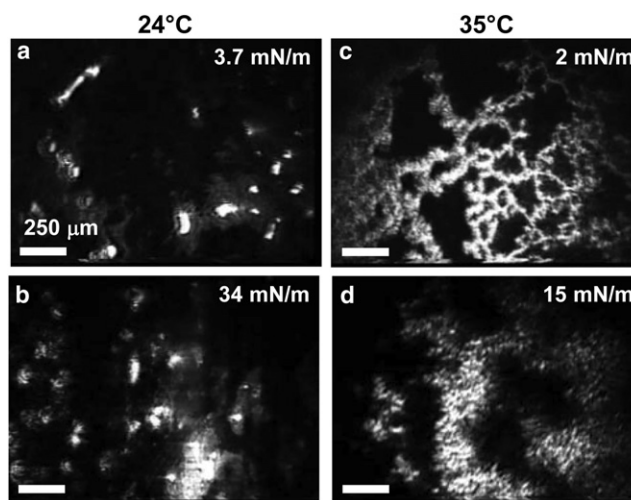


FIGURE 2 BAM images of an interfacial meibum film at 24°C at low surface pressure, 3.7 mN/m, (*a*) and high, 34 mN/m (*b*). The same meibum film at 35°C is shown at the same levels of compression, although the resultant surface pressures were 2 mN/m (*c*) and 15 mN/m (*d*). The mean molecular area of panel *c* is equivalent to panel *a* while the film in panel *d* is at equivalent compression to panel *b*. The scale bars are 250 μm.

be evidence of the reduced ability of meibum to pack efficiently at higher temperatures, presumably because, as the film was heated, a greater portion of the hydrocarbon chains occupied the *gauche* rotomers than the *trans* (19).

Interfacial rheology

These differences in microstructure of meibum resulted in vast changes in the interfacial viscoelastic properties as the film was heated. Shown in Fig. 3 is a representative sample with particularly high modulus values. At 17°C and 21 mN/m, the film was quite elastic ($G' > G''$) with high modulus values near 10 mN/m. As the film was heated, the interfacial moduli decreased. Between 26 and 30°C, the interfacial elastic modulus dropped quickly and the film became primarily fluid ($G'' > G'$) at ~27°C. At 35°C, the interfacial viscous modulus was at the sensitivity limit for the ISR (0.02 mN/m). This value represented a decrease in interfacial viscous modulus by greater than two orders of magnitude between 17 and 35°C. Meibum samples from multiple individuals were tested and all samples showed the same qualitative behavior: decrease in interfacial viscous and elastic moduli as the surface temperature increased. In all cases, the high temperature/low viscosity measurements were limited by the sensitivity of the ISR.

SAXS

SAXS was recorded for 10 samples at several temperatures between 25 and 40°C. A representative diffraction pattern is shown in Fig. 4. Evidence of a number of peaks are seen at different scattering vectors, q ; a summary of the prevalence of each peak as well as the d-spacings is given in Table 1. All samples contained at least one lipid phase with lamellar packing, represented by first- and second-order peaks (peaks

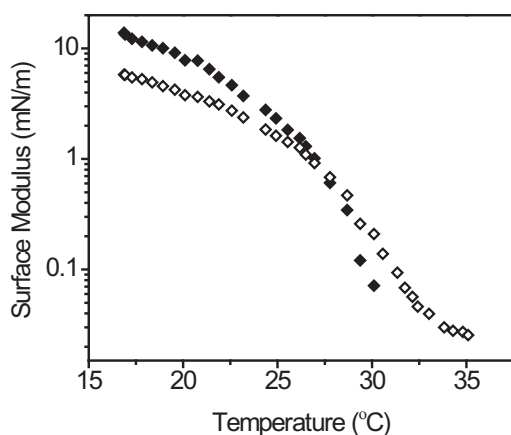


FIGURE 3 Dependence of interfacial viscoelasticity on temperature for a representative meibomian lipid film. The film was initially compressed to 21 mN/m at 17°C, then surface area was held constant as the film was heated. (Solid symbols) Elastic modulus, G' ; (open symbols) viscous modulus, G'' .

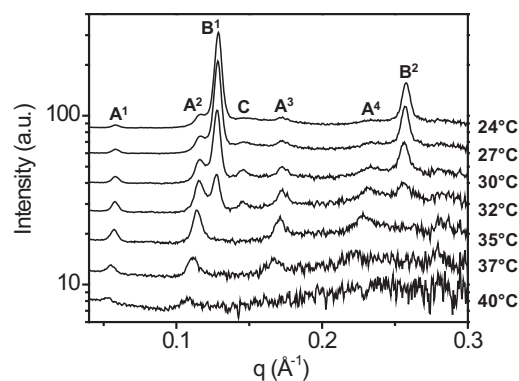


FIGURE 4 SAXS diffraction patterns of a representative meibum sample containing crystalline structures. Scattering at multiple temperatures between 24 and 40°C is shown. Peaks representing unique phases are lettered A–C, while the superscripts above the peak labels denote the order of the peak (1st–4th). Three phases with distinct d-spacings were observed: peak A at 0.057 \AA^{-1} , peak B at 0.129 \AA^{-1} , and peak C at 0.145 \AA^{-1} . Peak B was present in all 10 samples; peaks A and C were present in some samples. The results are summarized in Table 1.

B^1 and B^2) at q of $0.129 \pm 0.001 \text{ \AA}^{-1}$ and $0.257 \pm 0.003 \text{ \AA}^{-1}$ (average \pm standard deviation of 10 samples) corresponding to $48.8 \pm 0.52 \text{ \AA}$. The intensity of peak B decayed linearly with temperature (Fig. 5). For each sample, the linear fit was extrapolated to zero intensity to reveal the melt temperature; the average of all samples was $33.8 \pm 1.2^\circ\text{C}$. These structures represent lipids aligned by lamellar packing. This phase with a d-spacing of 49 Å will be referred to as the “majority” phase. Similar structures have been identified in other natural lipid systems such as skin lipids and lipids extracted from wool (29,30). After one heat cycle, the diffraction of three samples was measured a second time. Although peaks were present in the same locations and no new peaks were observed, the integrated intensity of the peak B^1 decreased in all three samples by as much as 50%, indicating a reduction in the prevalence of this phase after a heat cycle.

In addition to the majority phase represented by peak B, five of 10 samples contained a peak with a slightly shorter d-spacing, labeled peak C in Fig. 4. The d-spacing of peak C was 43 Å and this peak melted at the same temperature as peak B: between 32 and 35°C, although the intensity of this peak was too small to determine an accurate melt temperature. The intensity ratio of peak C to peak B^1 was not consistent between samples, but the common melt temperature suggests that peaks B and C could be related. One possibility is that peak C represents a second length scale

TABLE 1 Prevalence, d-spacing, and melt temperature of lamellar phases in meibum

	Prevalence	$d \pm (\text{Å})$	$T_m + (^\circ\text{C})$
Peak A	8/10	110.6 ± 2.3	40–42
Peak B	10/10	48.8 ± 0.53	33.8 ± 1.1
Peak C	5/10	43.4 ± 0.43	32–35

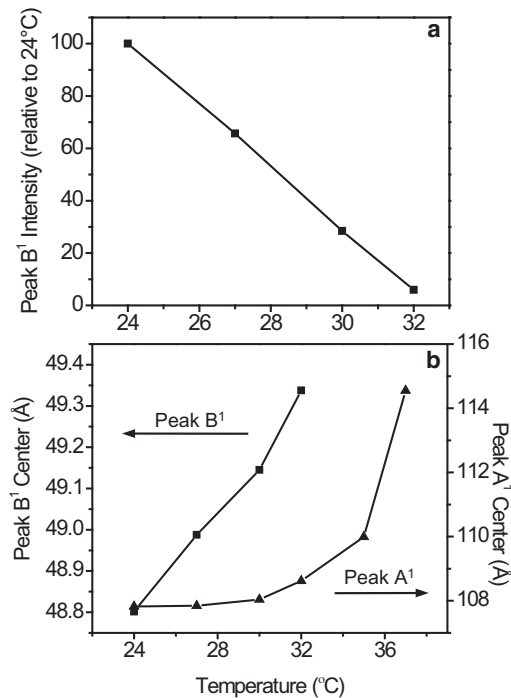


FIGURE 5 Intensity of peak B^1 decreased linearly with temperature as the majority phase melted. The center spacing of this peak also showed a linear dependence on temperature, in contrast to peak A^1 , which expanded nonlinearly. The increase in the spacing of peaks A and B is indicative of thermal expansion of the lamellar phases as they melted. Representative data from one sample are shown.

affiliated with the majority phase. However, this would be more likely if the presence of peak C correlated with high intensity of peak B , which was not the case. Another possibility is that peak C represents a distinct lamellar phase with shorter spacings that coincidentally melts at the same temperature as the majority phase.

Finally, diffraction patterns in eight of 10 samples indicated the presence of an additional structure with spacing at $110.6 \pm 2.3 \text{ \AA}$. Denoted peak A in Fig. 4, up to fourth-order peaks were observed, but the intensity of this peak was small compared to peak B . In three samples, the intensity of peak A was too small to achieve accurate Gaussian fits; therefore, the average value reported in Table 1 represents only five samples. In addition, in all samples the intensity of the second-order peak (A^2) was greater than the first-order peak (A^1). This minority phase with longer lamellar spacing melted at a higher temperature than the majority phase; peak A was present at temperatures as high as 40°C . The distinct melt temperature shows that 110 \AA represents the spacing of a unique phase, and the low intensity of peak A relative to peak B indicates that this was a less prevalent or secondary structure, therefore it will be referred to as the “minority” phase.

Peaks A and B showed different thermal behavior (Fig. 5). As the samples were heated, the intensity of peak B decreased linearly with temperature (Fig. 5 *a*). The

spacing of peak B also exhibited linear dependence on temperature as the majority phase underwent thermal expansion (Fig. 5 *b*). The increase in lamellar spacing was $<1 \text{ \AA}$ between 24 and 32°C . The length scale of peak A also increased with temperature, but it did so nonlinearly, with a total expansion of $\sim 6 \text{ \AA}$ (Fig. 5 *b*). These unique melt behaviors were consistent for each peak in all samples. Differences in melt behavior between the two structures may be an indication that the two phases are composed of distinct lipid species.

DISCUSSION

The dramatic dependence of interfacial rheological properties on temperature is directly applicable to meibum behavior in the eye. In a healthy eye, low viscosity at body temperature would facilitate expression of meibum from the glands and spreading of fresh lipids onto the tear-film surface. Once meibum arrives on the ocular surface, the average temperature of which has been reported to be between 33.8 and 34.3°C (31), lipids cool causing the interfacial elasticity of the film to increase. If mechanical integrity of the lipid layer is indeed linked to tear-film stability, small changes in meibum melt temperature could detrimentally influence both lipid layer performance and lipid secretion levels.

An essential property of meibum is the ability to be expressed from the glands onto the surface of the eye. If a disease state caused composition changes that increased meibum melt temperature, meibum viscosity would be enhanced at body temperature. Because gland expression requires the application of pressure to the eyelids by a blink, increased meibum viscosity could inhibit delivery of lipids to the tear film. Evaporation reduction is thought to be a major function of the lipid layer; therefore, another consequence of reduced lipid delivery would be increased evaporation of the aqueous layer (32). Such a mechanism has been long suspected to be a major cause of clinical symptoms in MGD, a disease state where the meibum becomes thicker through keratinization, often resulting in occluded meibomian glands and poor meibum delivery (33,34). Borchman et al. (8) have used infrared spectroscopy to demonstrate that meibum melt temperature in meibomian-gland-dysfunction patients is higher than in control patients. Although increased meibum viscosity has been suggested as an outcome of a higher melt temperature, this report is, to our knowledge, the first to quantify how dramatically meibum film viscosity changes with temperature within the melting region.

A more subtle consequence of altered meibum melt temperature is the stabilization of the lipid layer of the tear film. Surface elasticity has been shown to influence the dynamic wetting behavior of droplets (35); thus, dramatic changes of lipid layer viscosity could alter the ability of the lipid layer to spread after a blink, in addition to

modulating the propagation of dewetting phenomena in dry eye disease. At this point, the ideal mechanical properties necessary to stabilize the tear film remain unknown.

In addition to exhibiting remarkable interfacial rheological properties, the changes in surface pressure versus area isotherms with temperature of meibum were unusual compared to most lipids. A number of lipids, including sphingolipids, phospholipids, and fatty acids, effectively expand upon heating (36–38). The isotherms of more conventional lipids at high temperatures exhibit greater surface pressures at similar areas compared to colder temperatures. In contrast, the surface pressure of meibum films at 24°C was much higher than at 35°C, and similar results in chloroform-spread meibum have been reported by Millar and Mudgil (39). Meibum is an unusual material, and there are several factors that may contribute to seemingly unusual behavior by mean molecular area.

Most meibomian lipids are more hydrophobic than traditional monolayers. The hydrocarbon chains for most lipids found in meibum are quite long, and at low surface pressures the lipids have a tendency to aggregate rather than spread evenly across the surface (Fig. 2 a). At lower temperatures, the boundaries of these islands of material should be more rigid than at higher temperatures. Thus, until the interface is fully covered with material, compression of the film would push islands of material together rather than rearranging meibum on a molecular scale. This would effectively cause meibum at colder temperatures to take up more space, resulting in higher surface pressures. When heated to 35°C, the lipids and island boundaries are more fluid. At these higher temperatures, meibum behavior may be akin to traditional lipid behavior. Related to this notion, such islands may contain multiple layers of lipids, and the degree of multilayer formation may depend on compression level. Even in solvent-spread films, the estimated mean molecular areas of meibomian lipid films have suggested that meibum easily forms multilayers (39).

In addition, the spreading of lipids without solvent may result in fundamentally different organization compared to monolayers traditionally spread from chloroform. But, isotherms of solvent spread and neat meibum films are similarly featureless, making interpretations beyond molecular area comparisons difficult. Additional work has shown that interfacial meibum films spread neat or from chloroform or hexane solutions achieve similar interfacial rheological properties (see [Supporting Material](#)), indicating that altered molecular organization may not strongly influence macroscopic properties. Investigation of molecular structure via interfacial x-ray scattering techniques may be required to fully elucidate structural differences.

Although structures formed by meibum at the air-water interface will not be exactly the same as structures found in the bulk sample by SAXS, comparing results from both experiments gives some insight into how meibum structure and rheology are related. We have shown that meibum is

a structured material with high interfacial viscoelasticity at room temperature, but when heated to body temperature the majority phase melted and the viscosity of interfacial meibum films was greatly reduced. BAM images also suggested that the lipids became more disordered when heated from 24°C to 35°C, which could be responsible for the decrease in overall surface viscosity. The major transition in interfacial viscosity occurred between 20 and 30°C while the temperatures at which the bulk lamellar phases melted were elevated. The majority phase (peak B) melted between 32 and 35°C, whereas the secondary phase found in some samples (peak A) persisted up to 40°C. Similar reduction of melt temperature in interfacial films compared to bulk samples has been previously reported in confined polymer films (40).

The lipid layer of the tear film is estimated to be ~20 molecules thick (6), thus meibum in the lipid layer may be best described as a bulk material. However, the water interface can still influence meibum organization. Even in thick multilayer films, the layers nearest the interface can show low-dimensionality behavior, or organization induced by contact with the interface (41). Therefore, both the interfacial and bulk properties reported here will be relevant to the lipid layer of the tear film, and we expect that melt transitions and physical structures of meibomian lipids in the lipid layer of the tear film will lie somewhere between those of bulk meibum and interfacial films.

Because SAXS is quantitative, it may be a valuable tool for identifying changes in meibum properties that occur with disease. The sample-to-sample variation of the spacing in each of the three peaks identified by SAXS was remarkably low and the melt behavior of these peaks was the same in all samples within 1°C. Therefore, we hypothesize that the majority and minority phases identified by SAXS were each composed of a specific lipid or set of lipids with characteristic chain lengths. These lipids would be commonly produced among individuals and would have a natural tendency to form ordered structures. Although it is impossible at this time to identify which lipids were present in these phases, comparisons can be made to other mixed lipid systems. Skin lipids and wool lipids are primarily composed of ceramides and fatty acids, and these natural lipid mixtures form lamellar structures with spacings similar to meibum. In wool lipid mixtures, phases have been identified with spacings of 54 and 47 Å. These were thought to consist of bilayers of C18–C24 ceramides and C16–C18 free fatty acids, respectively (30). Perhaps more similar to meibum, stratum corneum (skin) lipids organize into two major structures with lamellar spacings of 62 and 130 Å (29). Synthetic mixtures of fatty acids, cholesterol, and ceramides were able to reproduce the dual phase behavior, suggesting that an optimal variation of hydrocarbon chain lengths exists to produce both long and short periodicity phases in such mixtures (42).

Lipids with hydrocarbon chains 18–30 carbons long are some of the major constituents of meibum (16,17), which

may reasonably form the short periodicity (49 Å) structures. The lipids responsible for forming structures with 110 Å lamellar spacing are more difficult to determine, as these would require quite long hydrocarbon chains or bilayers of lipids (29). Using HPLC-mass spectrometric analysis, Butovich et al. (16) have identified cholesterol esters as a source for very long chains in human meibum. Cholesterol esters with hydrocarbon chains as long as 34 carbons have been confirmed, with the possibility that such species with even longer chains are present (17). Or, rather than cholesterol esters, the minority phase could consist of extended wax esters, although the chains would need to be quite long (21,43). The intensity of the A² peak was stronger than the A¹ peak, which is consistent with scattering from a bilayer, in which case the molecules would be roughly 55 Å long.

Although the 110 Å phase was less prevalent than the 49 Å phase, SAXS results indicated that the minority phase would be present under physiological conditions, whereas the majority phase would be melted. Thus, the prevalence of the minority lamellar phase could influence meibum performance in the eye, and the presence or absence of this phase may be indicative of compositional differences between the samples. With a melt temperature above 40°C, the minority phase will exist in the meibomian glands and it may be enhanced upon secretion onto the lipid layer of the tear film, which is estimated to be a few degrees cooler than body temperature (average values are reported near 34°C with spatial variations) (31). The melting of all lamellar phases above 40°C also corresponds nicely with visual observations that meibum appears to transition from solid to liquid above 40°C (44,45), as structure is typically correlated with high viscosity or elasticity. The minority phase was not observed in all meibum samples; meibum without this phase may be liquid crystalline or amorphous under physiological conditions. The physical organization of lipids excluded from the lamellar phases has yet to be determined.

CONCLUSION

We have shown that there is a relationship between structure and mechanical properties of meibomian lipids, and that these vary greatly within the previously reported melt range, 20–40°C (19,44,45). Interfacial rheological properties decreased by several orders of magnitude within this temperature range, identifying a mechanism through which composition changes could influence lipid performance. Evidence of lamellar phases was found in all samples through small angle x-ray scattering. A structure with spacings at 49 Å that melted near 33°C was identified in all meibum samples while some samples also contained structures with 110 Å spacing that melted above 40°C. Clinical differentiation between healthy and disease states such as dry eye or MGD has been hindered, to date, due to the lack of objective tests. The quantitative nature of SAXS and the consis-

tency between samples in this preliminary study of healthy meibum provides support for further exploration of this method. Because meibum structure is responsible for viscoelasticity and both are sensitive to temperature, meibum melt temperature may be critical for meibum expression and tear-film stabilization mechanisms in vivo.

SUPPORTING MATERIAL

Four figures are available at [http://www.biophysj.org/biophysj/supplemental/S0006-3495\(11\)05419-1](http://www.biophysj.org/biophysj/supplemental/S0006-3495(11)05419-1).

Portions of this research were carried out at the Stanford Synchrotron Radiation Lightsource, a Directorate of Stanford Linear Accelerator Center National Accelerator Laboratory and an Office of Science User Facility operated for the U.S. Department of Energy Office of Science by Stanford University. We thank John Pople for help conducting the SAXS experiments.

The authors are grateful to the American Physical Society for supplying a grant through the India-U.S. Physics Student Visitation Program that enabled conduction of preliminary SAXS experiments at the IISc, Bangalore in the lab of Jaydeep Basu along with Sunita Srivistava and Sivasunder C. In addition, this work was supported by Alcon Research and a Stanford Graduate Fellowship. Michelle Senchyna, Howard Ketelson, and David Meadows are employees of Alcon Research.

REFERENCES

- Holly, F. J. 1973. Formation and rupture of the tear film. *Exp. Eye Res.* 15:515–525.
- Sharma, A., and E. Ruckenstein. 1985. Mechanism of tear film rupture and formation of dry spots on cornea. *J. Coll. Int. Sci.* 106:12–27.
- Wong, H., I. Fatt, I., and C. J. Radke. 1996. Deposition and thinning of the human tear film. *J. Colloid Interface Sci.* 184:44–51.
- Pflugfelder, S. C., A. Solomon, and M. E. Stern. 2000. The diagnosis and management of dry eye: a twenty-five-year review. *Cornea.* 19:644–649.
- Bron, A. J., J. M. Tiffany, ..., L. W. Voon. 2004. Functional aspects of the tear film lipid layer. *Exp. Eye Res.* 78:347–360.
- Butovich, I. A., T. J. Millar, and B. M. Ham. 2008. Understanding and analyzing meibomian lipids—a review. *Curr. Eye Res.* 33:405–420.
- Ohashi, Y., M. Dogru, and K. Tsubota. 2006. Laboratory findings in tear fluid analysis. *Clin. Chim. Acta.* 369:17–28.
- Borchman, D., M. C. Yappert, and G. N. Foulks. 2010. Changes in human meibum lipid with meibomian gland dysfunction using principal component analysis. *Exp. Eye Res.* 91:246–256.
- Khanal, S., A. Tomlinson, ..., K. Ramaesh. 2008. Dry eye diagnosis. *Invest. Ophthalmol. Vis. Sci.* 49:1407–1414.
- Shine, W. E., and J. P. McCulley. 1991. The role of cholesterol in chronic blepharitis. *Invest. Ophthalmol. Vis. Sci.* 32:2272–2280.
- Tiffany, J. M. 2003. Tears in health and disease. *Eye (Lond.).* 17:923–926.
- Souchier, M., C. Joffre, ..., C. Creuzot-Garcher. 2008. Changes in meibomian fatty acids and clinical signs in patients with meibomian gland dysfunction after minocycline treatment. *Br. J. Ophthalmol.* 92:819–822.
- Goto, E., and S. C. G. Tseng. 2003. Kinetic analysis of tear interference images in aqueous tear deficiency dry eye before and after punctal occlusion. *Invest. Ophthalmol. Vis. Sci.* 44:1897–1905.
- Yokoi, N., H. Yamada, ..., S. Kinoshita. 2008. Rheology of tear film lipid layer spread in normal and aqueous tear-deficient dry eyes. *Invest. Ophthalmol. Vis. Sci.* 49:5319–5324.

15. Blackie, C. A., J. D. Solomon, ..., D. R. Korb. 2009. The relationship between dry eye symptoms and lipid layer thickness. *Cornea*. 28:789–794.
16. Butovich, I. A., E. Uchiyama, and J. P. McCulley. 2007. Lipids of human meibum: mass-spectrometric analysis and structural elucidation. *J. Lipid Res.* 48:2220–2235.
17. Butovich, I. A. 2009. Cholesteryl esters as a depot for very long chain fatty acids in human meibum. *J. Lipid Res.* 50:501–513.
18. Chen, J., K. B. Green-Church, and K. K. Nichols. 2010. Shotgun lipidomic analysis of human meibomian gland secretions with electrospray ionization tandem mass spectrometry. *Invest. Ophthalmol. Vis. Sci.* 51:6220–6231.
19. Borchman, D., G. N. Foulks, ..., D. V. Ho. 2007. Temperature-induced conformational changes in human tearlipids hydrocarbon chains. *Biopolymers*. 87:124–133.
20. Borchman, D., G. N. Foulks, ..., E. Schwietz. 2010. Physical changes in human meibum with age as measured by infrared spectroscopy. *Ophthalm. Res.* 44:34–42.
21. Borchman, D., G. N. Foulks, ..., V. Greenstone. 2011. Human meibum lipid conformation and thermodynamic changes with meibomian-gland dysfunction. *Invest. Ophthalmol. Vis. Sci.* 52:3805–3817.
22. Schein, O. D., J. M. Tielsch, ..., S. West. 1997. Relation between signs and symptoms of dry eye in the elderly. A population-based perspective. *Ophthalmology*. 104:1395–1401.
23. Millar, T. J., S. T. Tragoulias, ..., P. Mudgil. 2006. The surface activity of purified ocular mucin at the air–liquid interface and interactions with meibomian lipids. *Cornea*. 25:91–100.
24. Brooks, C. F., G. G. Fuller, ..., C. R. Robertson. 1999. An interfacial stress rheometer to study rheological transitions in monolayers at the air–water interface. *Langmuir*. 15:2450–2459.
25. Reynaert, S., C. F. Brooks, ..., G. G. Fuller. 2008. Analysis of the magnetic rod interfacial stress rheometer. *J. Rheol.* 52:261–285.
26. Haworth, K. M., J. J. Nichols, ..., K. K. Nichols. 2011. Examination of human meibum collection and extraction techniques. *Optom. Vis. Sci.* 88:525–533.
27. Hénon, S., and J. Meunier. 1991. Microscope at the Brewster angle: direct observation of first-order phase transitions in monolayers. *Rev. Sci. Instrum.* 62:936–939.
28. Leiske, D. L., S. R. Raju, ..., G. G. Fuller. 2010. The interfacial viscoelastic properties and structures of human and animal Meibomian lipids. *Exp. Eye Res.* 90:598–604.
29. McIntosh, T. J., M. E. Stewart, and D. T. Downing. 1996. X-ray diffraction analysis of isolated skin lipids: reconstitution of intercellular lipid domains. *Biochemistry*. 35:3649–3653.
30. Fonollosa, J., L. Campos, ..., L. Coderch. 2004. X-ray diffraction analysis of internal wool lipids. *Chem. Phys. Lipids*. 130:159–166.
31. Tan, J. H., E. Y. K. Ng, and U. R. Acharya. 2011. Evaluation of topographical variations in ocular surface temperature by functional infrared thermography. *Infrared Phys. Technol.* 54:467–477.
32. Mathers, W. 2004. Evaporation from the ocular surface. *Exp. Eye Res.* 78:389–394.
33. Green-Church, K. B., I. Butovich, ..., B. J. Glasgow. 2011. The international workshop on meibomian gland dysfunction: report of the subcommittee on tear film lipids and lipid-protein interactions in health and disease. *Invest. Ophthalmol. Vis. Sci.* 52:1979–1993.
34. Gilbard, J. P., S. R. Rossi, and K. G. Heyda. 1989. Tear film and ocular surface changes after closure of the meibomian gland orifices in the rabbit. *Ophthalmology*. 96:1180–1186.
35. Leiske, D. L., C. Monteux, ..., G. G. Fuller. 2011. Influence of surface rheology on dynamic wetting of droplets coated with insoluble surfactants. *Soft Matter*. 10.1039/C1SM05231D.
36. Schwartz, D. K., M. L. Schlossman, and P. S. Pershan. 1992. Re-entrant appearances of phases in a relaxed Langmuir monolayer of tetracosanoic acid as determined by x-ray scattering. *J. Chem. Phys.* 96:2356–2370.
37. Li, X. M., J. M. Smaby, ..., R. E. Brown. 2000. Sphingomyelin interfacial behavior: the impact of changing acyl chain composition. *Biophys. J.* 78:1921–1931.
38. Garidel, P., and A. Blume. 2005. 1,2-Dimyristoyl-*sn*-glycero-3-phosphoglycerol (DMPG) monolayers: influence of temperature, pH, ionic strength and binding of alkaline earth cations. *Chem. Phys. Lipids*. 138:50–59.
39. Millar, T. J., and P. Mudgil. 2011. Surfactant properties of human meibomian lipids. *Invest. Ophthalmol. Vis. Sci.* 10–5445.
40. Forrest, J. 1997. Interface and chain confinement effects on the glass transition temperature of thin polymer films. *Phys. Rev. E.* 56:5705–5716.
41. Gupta, A., P. Rajput, ..., H. Amenitsch. 2008. Low-dimensionality effects in the melting of a Langmuir-Blodgett multilayer. *Langmuir*. 24:7793–7796.
42. de Jager, M. W., G. S. Gooris, ..., J. A. Bouwstra. 2005. Lipid mixtures prepared with well-defined synthetic ceramides closely mimic the unique stratum corneum lipid phase behavior. *J. Lipid Res.* 46:2649–2656.
43. Kreger, D. R., and C. Schamhart. 1956. On the long crystal-spacings in wax esters and their value in micro-analysis of plant cuticle waxes. *Biochim. Biophys. Acta.* 19:22–44.
44. Linton, R. G., D. H. Curnow, and W. J. Riley. 1961. The meibomian glands. *Br. J. Ophthalmol.* 45:718–723.
45. Brown, S. I., and D. G. Dervichian. 1969. The oils of the meibomian glands. Physical and surface characteristics. *Arch. Ophthalmol.* 82:537–540.